A Method For On-Board Fire Detection Based On The Integration Of Expert Systems And Neural Networks

WANG Fuhai[1,*], YUE Ronggang[1], SUN Rongyang[1], LIU Fengjing[1], and KONG Xianghao[1]

[1]Institute of Remote Sensing Satellite, CAST, 100094. Beijing China
[*]hitwfh@163.com

Keywords: On-board intelligent processing, Fire detection, Feature map, Multi-source data fusion processing.

Abstract

Fire accidents (especially large-scale fires) pose significant threats to human society, such as forest fires and chemical plant explosions, which can cause substantial loss of life, health, and economic damage. However, current fire detection using remote sensing satellites is mostly for post-disaster confirmation rather than pre-disaster warning, lacking a high-timeliness, high-accuracy onboard fire detection and warning scheme. On the other hand, the significant improvement in satellite payload technology and the increasing richness of satellite remote sensing data products have made the processing of remote sensing data products increasingly difficult. In fire detection, the satellite detection scheme determines the satellite's application capability and further determines whether the satellite can maximize its effectiveness. Based on the intelligent detection application requirements for onboard fire targets, this paper focuses on solving the problems of the existing fire detection models, such as the difficulty in eliminating high-reflective objects and other false fire targets, the large data volume when using multi-band combinations that cannot ensure onboard processing timeliness, and the poor environmental adaptability of existing fire detection schemes. A high-timeliness, high-confidence, and highly adaptable high-orbit satellite multi-spectral onboard fire intelligent detection scheme is proposed. By integrating expert system feature maps for fire confirmation, the scheme meets the high-frequency inspection and rapid warning needs for fires, supporting the integrated application of satellite and ground systems, and will significantly enhance the early warning detection efficiency of satellite fire detection.

1. Instruction

In recent years, global climate change has intensified the frequency of forest fires, posing severe threats to ecosystems and human society. For instance, the 2019 Australian bushfires burned 11.7 million square kilometers of land, causing direct economic losses exceeding $5 billion and the death or displacement of billions of animals (Van Oldenborgh, G., J., et al., 2020). These events underscore the limitations of conventional fire monitoring methods, such as restricted coverage of manual inspections, delayed response times, and observation tower is greatly restricted by terrain (Zhang, F., et al., 2020).

Figure 1. Satellite image of Melbourne during the Australian bushfires.

Satellite remote sensing technology, with its advantages of wide-area coverage and real-time dynamics, provides a new technical approach for early fire warning. Remote sensing satellites can achieve large-scale continuous monitoring, and their multispectral imaging capabilities can effectively capture fire characteristics (Wang, J., H., et al., 2022). However, satellite-based fire detection still faces several technological challenges:

High false alarm rate: Industrial heat sources (such as steel plants and coal-fired power plants) exhibit thermal radiation characteristics similar to real fires, resulting in a high false alarm rate.

Massive multispectral data: The large amount of multispectral data from remote sensing satellites makes it difficult for existing processing architectures to meet real-time detection requirements.

Dynamic background changes: Factors such as diurnal variation and seasonal variations lead to dynamic changes in background features, resulting in poor robustness of fixed threshold detection methods (Ding, Y., et al., 2023).

Therefore, there is an urgent need to develop an airborne multispectral fire detection solution with high timeliness, reliability, and adaptability.

2. Research Status

In recent years, deep learning algorithm has been widely concerned and applied in the field of remote sensing image fire

detection. Traditional methods such as fire point detection based on threshold judgment have problems such as poor environmental adaptability and difficult threshold selection, which are difficult to meet the complex and changeable fire monitoring needs. By automatically extracting features, the deep learning algorithm can deeply mine the information of remote sensing data, has a better ability to analyze remote sensing images, and can play an important role in fire detection.

Convolutional neural networks (CNNs) are outstanding in automatic feature extraction and improve the detection accuracy. Gargiulo (Gargiulo, M., et al., 2019) used super-resolution CNN on sentinel-2 images to improve small target detection. Dell'aglio (Dell'aglio, D., A., G., et al., 2019) proposed a multi-scale CNN architecture combining active fire index (AFI) and near infrared band data, which further improved the accuracy..

In terms of instance segmentation, Mask R-CNN proposed by Begum (Begum, S., R., et al., 2021) achieves pixel level segmentation through two-stage detection, but it suffers from high computational complexity. Chen (Chen, L., C., et al., 2018) introduced deeplabv3+ with a characteristic pyramid network to enhance semantic information and reduce computational costs, however, real-time performance remains a challenge.

In summary, designing high-precision and lightweight neural networks, and applying them to real-time monitoring of fire targets in remote sensing images, enables rapid and accurate detection of fire flames. This provides strong support for fire early warning and emergency response.

3. Methodology

3.1 Spectral Band Optimization for Efficient Fire Detection

Using a signal-to-clutter ratio (SCR) calculation model, the SCR of fire targets under different types and scenarios is computed, and normalized SCR projection maps across spectral bands are plotted. The intersection of spectral bands with peak SCR values is identified by analyzing SCR projections of different target-scenario combinations. As shown in Figure 2, spectral band optimization is performed to select the range of spectral bands with higher SCR values for all targets and scenarios as the preferred spectral bands.

Figure 2. Spectral band optimization process.

First, the SCR of the target in different background regions is calculated, and the spectral bands corresponding to the relative peak SCR regions are selected as the initial candidates. Then, within the initially selected spectral bands, SCR projection maps for different central wavelengths and bandwidths are plotted to identify the spectral bands that exhibit higher SCR values for various targets across different scenarios as the candidate detection bands. Next, within the candidate bands, the impact of various factors on target detectability is analyzed. The sensitivity requirements for the detector are provided, and the SCR of the candidate band images is analyzed based on these requirements. Finally, the optimal spectral bands for target detection are determined.

Taking typical forest fire, grassland fire and other targets as examples, the detectability of targets in the selected spectral segment is analyzed, and the difference of detectability between the selected spectral segment and other unselected spectral segments is compared to verify the rationality of the selected spectral segment.

The detectability of the target reflects the energy difference between the target and the background physically. In the process of target detection, clutter is often difficult to deal with. Therefore, to establish the target detectability characterization model, it is necessary to quantitatively characterize the spatial clutter. Based on the background clutter quantitative characterization model, combined with the signal to clutter ratio model, the target detectability characterization model is established. This model is used to analyze the detectability of aerial targets, and combined with the sensitivity characteristics of the detection system, the alternative suggestions of target detection spectrum are given.

When calculating the background clutter intensity, multiple regions are randomly selected within the background, and the mean square deviation within each region is calculated separately. The average value is then taken to obtain the overall clutter fluctuation of the background. The method for selecting clutter calculation regions is illustrated in Figure 3.

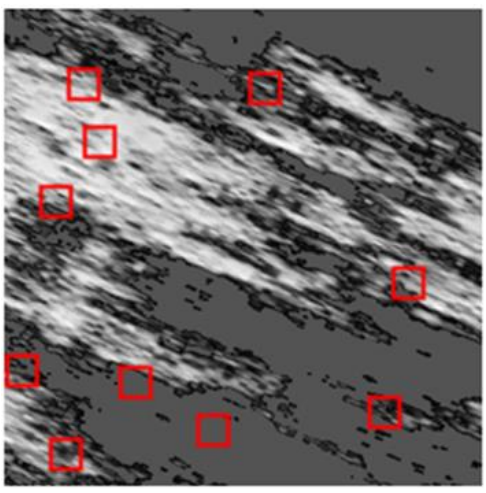

Figure 3. Background clutter sampling regions.

The premise that the target can be detected by the detector is that there is a certain degree of difference between the target and the background. Based on the background clutter quantization model, a representation model of the detectability

of target is established based on the maximization of the difference between the target and the background, which is defined as:

$$SCR_{tar} = \frac{|\mu_T - \mu_B|}{C}, \quad (1)$$

where SCR_{tar} = target SCR
μ_T = target energy (point target energy)
μ_B = background energy
C = spatial clutter metric

Based on the aforementioned characterization model and the data of target and background characteristics, the detectability analysis of targets and the optimal band selection can be conducted. By analyzing the detectability of different combinations of targets and clutter intensities, a suitable set of detection bands can be determined. The size of this set can be controlled by setting a target SCR threshold. Points that exceed this threshold are considered candidate bands. From these candidate bands, the point with the highest SCR is selected as the optimal working band, which includes the central wavelength and spectral bandwidth.

3.2 Expert System-Based Feature Atlas Construction

Due to the interference caused by the background in fire point detection, distinguishing fire points from the background in remote sensing images remains a critical challenge that urgently needs to be addressed. The traditional method uses the single feature "Brightness" of the image as the fire point detection criterion, which is vulnerable to the influence of environmental temperature and other factors, resulting in false alarm. Therefore, it is necessary to increase the dimension of the feature quantity involved in the fire point detection criterion to improve the accuracy of fire point detection. However, the existing fire point characteristics data mining for different regions, different wind zones, different features and so on is not complete, and the feature quantity is extremely lacking.

Based on multi-source remote sensing data information mining, this paper collects the characteristics of the fire point, including the temporal and spatial characteristics of the flame, the seasonal characteristics of the flame, the spectral characteristics of the flame, and the difference between the fire point and the background temperature. The known part of the data is classified, and the fire points of different time-space spectral segments are obtained. This part of the data is used as a priori knowledge. By analyzing the characteristics of remote sensing data, the fire point characteristics based on image data are obtained. According to the characteristic information of flame direction, shape, spectrum, smoke color, texture, size, global and local spatial geometry, the information integration is completed, and the fire point type data sets with different spatio-temporal feature maps are obtained.

Color Features: Statistical metrics such as color histograms, mean values, and color entropy are used to quantify color characteristics.

Spatial Information: Target positions are derived from image coordinate systems. Small targets are represented as point coordinates, while larger targets are represented as multi-point or polygonal regions.

Spectral Features: Reflect the physical properties of surface objects. Band mean and standard deviation are used to extract spectral features:

$$spe = [mean,\ std]$$
$$\text{mean} = \frac{\sum_{i=1}^{n} v_i}{n}$$
$$std = \sqrt{\frac{\sum_{i=1}^{n} (v_i - mean)^2}{n}}, \quad (2)$$

where n = the number of pixels per grid
v_i = the grayscale value of the i-th pixel

Texture Features: Reflect the periodic structural arrangement of surface objects. Local Binary Patterns (LBP) are employed to extract local texture features. LBP is a texture descriptor with grayscale and rotation invariance. A 3×3 window is defined, with the center pixel's grayscale value as the threshold. Adjacent pixels are compared to the threshold, generating an 8-bit binary code for each center pixel:

$$LBP(x_c, y_c) = \sum_{p=1}^{8} s(I(p) - I(c)) \times 2^p, \quad (3)$$

where $I(p)$ = gray value of the p-th pixel except for the window pixel
$I(c)$ = gray value of center pixel.

If $s(I(p) - I(c)) \geq 0$, it is 1, otherwise it is 0. Traverse all pixels in the window to get an 8-bit binary number as the LBP eigenvalue of the central pixel.

Geometric features, this study employs the Speeded Up Robust Features (SURF) operator and the Evaluation of GIST (GIST) operator to extract local and global geometric features from the images, respectively. SURF is a local feature descriptor capable of overcoming the limitations of traditional geometric feature descriptions, such as affine transformations, lighting variations, and 3D viewpoint changes, to extract local geometric features from images. To ensure scale invariance, the algorithm first applies box filtering to the grid using different template sizes, constructing a pyramid of images with multi-scale blob responses. The positions of feature points at different scales are then determined using the Hessian matrix determinant, as described by the following formula:

$$\det(H) = \frac{\partial^2}{\partial x^2}\frac{\partial^2 f}{\partial y^2} - \left(\frac{\partial^2 f}{\partial x \partial y}\right), \quad (4)$$

where x, y = the horizontal and vertical coordinates of the pixel
$f(x, y)$ = pixel value at that point

When the Hessian matrix determinant reaches a local maximum, the corresponding point is identified as a feature point.

3.3 Lightweight On-Board Fire Detection Framework

A labeled dataset is constructed using publicly available remote sensing imager, with annotations performed manually or through technical means. The dataset undergoes preprocessing, including denoising, atmospheric correction, geometric rectification, and data augmentation, to enhance its quality and usability for training.

To reduce computational costs during feature extraction, a lightweight feature extraction network, MobileNetV2, is introduced to replace the Backbone of YOLOv5s. MobileNetV2 employs an inverted residual structure with linear bottlenecks to minimize computational overhead caused by excessive convolutional layers (Figure 4). The network first expands low-dimensional compressed representations into high-dimensional space, applies lightweight depthwise convolutions for filtering, and then projects the high-dimensional features back to low-dimensional compressed representations using a linear bottleneck function. Depthwise separable convolutions are utilized to reduce model parameters and computational load while maintaining high classification accuracy. These convolutions decompose standard convolutions into depthwise convolutions (applied independently to each input channel) and pointwise convolutions (combining outputs from depthwise convolutions), effectively suppressing parameter growth.

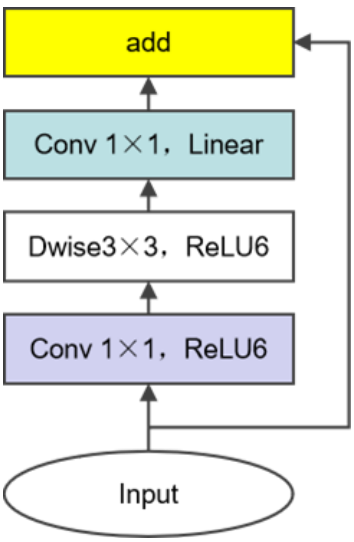

Figure 4. MobileNetV2 architecture.

To enhance feature extraction and ensure thorough model training, the original MobileNetV2 structure is optimized. The Mish activation function replaces ReLU6 due to its non-saturation and boundary-free properties, which improve gradient descent performance. The Mish function is defined as:

$$\mathrm{Mish}(x) = x\tanh\left(1+e^{x}\right), \tag{5}$$

where x = input features

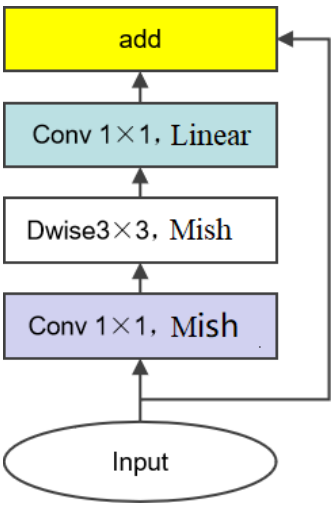

Figure 5. Optimized MobileNetV2 architecture.

After initial fire detection using the neural network, fire locations, types, and confidence levels are obtained. For each image, the fire type probability is represented as:

$$F_1 = \left\{(x_i, y_i), c_i, \left[(t_1, p_1), (t_2, p_2), \ldots, (t_n, p_n)\right]\right\}, \tag{6}$$

where i = the fire index

(x_i, y_i) = the latitude and longitude of the fire

c_i = the detection confidence level (influenced by factors such as cloud interference, location, solar elevation, and season)

p_i = the probability of fire type i

Furthermore, the feature maps are integrated to confirm fire points. Due to the limited on-board storage capacity of feature maps and the inability to fully cover all conditions such as latitude, longitude, solar elevation angle, season, and radiance during their construction, data gaps may occur when querying the feature maps based on on-orbit observation conditions. Therefore, data interpolation is required to retrieve feature map data.

Spatial interpolation methods are employed to predict values at unknown locations based on existing data, enabling the generation of continuous spatial surfaces. This approach is suitable for scenarios where variables such as latitude, longitude, and solar elevation angle are continuous during on-orbit observations. Using the query variables of the feature maps as spatial variables, Kriging interpolation is applied for spatial interpolation. Kriging interpolation considers the spatial autocorrelation between data points, handles data with various spatial distributions without requiring regularity in data distribution, and adaptively adjusts the interpolation results based on the density and distribution characteristics of the observed data. As a result, it is highly adaptable for interpolating feature maps in satellite-ground scenarios. The specific implementation process of Kriging interpolation is as follows:

Variogram Fitting: Based on the attribute values and spatial coordinates of known points, a variogram model is established. The variogram describes the spatial correlation between sample points, typically modeled using a Gaussian function.

Semi-Variogram Calculation: The semi-variogram is computed to quantify the differences between known points, determining the spatial correlation between sample points in the feature map.

Kriging Weight Calculation: Using the attributes, spatial coordinates, and semi-variogram of known points, the spatial weights between unknown points and known points are calculated.

Attribute Value Prediction: The attribute values of unknown points are predicted using the attribute values of known points and the Kriging weights, employing the ordinary Kriging method.

Through this process, fire type probabilities from the feature atlas are obtained:

$$F_2 = \left\{(x_i, y_i), \left[(t_1, p_1'), (t_2, p_2'), \ldots, (t_n, p_n')\right]\right\}, \quad (7)$$

In the expert system, feature atlas confidence f and image detection confidence $1-f$ are combined to confirm fire types:

$$F_3 = \left\{(x_i, y_i), \left\{(t''_n, p''_n = (1-f)c_i p_n + [1-(1-f)c_i]\, p_n')\right\}\right\}, \quad (8)$$

This fusion mechanism effectively reduces false alarms and improves detection accuracy.

During on-board operations, detected fire types from image detection, feature atlas, and expert system fusion F_1, F_2, F_3 are downlinked. Ground validation adjusts the feature atlas confidence f, enabling on-board model updates.

4. Experimental Validation

To comprehensively evaluate the system's performance, multiple sets of comparative experiments were designed. The experimental data were sourced from GF-4 satellite on-board imagery, covering various scenarios such as forests and grasslands, with a time span encompassing all four seasons. On each remote sensing image, 150 fire points were randomly added. To simulate real fire conditions, each fire point's temperature was randomly generated within the range of 500–1200 K, and its area was randomly set between 2–250 m².

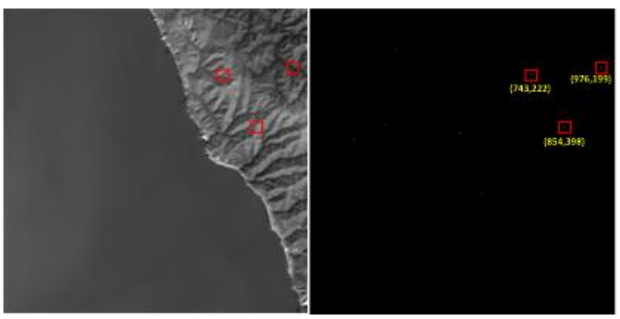

Figure 6. Detection result (SCR = 2).

In terms of detection accuracy, the proposed method achieved a mean Average Precision (mAP) of 92.3% on the test set. Compared to existing methods, it maintained high accuracy while significantly reducing the false alarm rate to less than 3%.

Real-time performance tests indicated that the system's processing latency was less than 10 seconds, with a data throughput of only 0.105 Gbit, meeting the requirements for on-board real-time processing. Environmental adaptability tests demonstrated that the system's detection accuracy fluctuated by less than 5% under different seasonal and diurnal conditions, showcasing strong robustness.

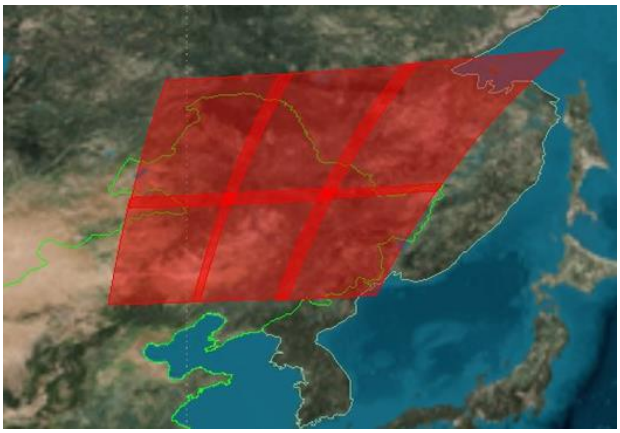

Figure 7. Forest Fire Patrol Plan for Northeast China's Forest Regions.

Taking China's largest Northeast Forest Region (covering 309,400 km², accounting for 37% of China's forest area) as an example, the proposed design can complete fire patrol and early warning for the entire region in 253 seconds. This significantly enhances the satellite's operational efficiency, enabling multiple daily patrols of key forest areas.

Process	Time
Single-area imaging	3s
On-board detection	10s
Data downlink	10s
Satellite maneuvering (in parallel with downlinking and processing.)	45s
Total	3*6+45*5+10=253s

Table 1. Timeliness

5. Conclusion

This paper proposes an on-board fire detection method that integrates expert systems with neural networks, with the main innovations including:

Construction of a Multi-Spectral Band Optimization Model: Through signal-to-clutter ratio analysis and target detectability evaluation, the optimal detection spectral bands were determined, significantly enhancing target detection performance.

Design of a Lightweight Detection Network Architecture: Utilizing an improved MobileNetV2 as the backbone, combined with the Mish activation function and a multi-task loss function, a balance between detection accuracy and real-time performance was achieved.

An expert system fusion mechanism was developed: by utilizing the semantic consistency among categories extracted from feature maps to interferometrically correct the confidence of output results, the false alarm rate was effectively reduced, and the system's robustness was improved.

Experimental results demonstrate that this method outperforms existing methods in terms of detection accuracy, real-time performance, and environmental adaptability, providing a new technical approach for real-time fire detection on satellites.

References

Begum S R, Datta S Y, Manoj M S V. Mask R-CNN For Fire Detection[J]. International Research Journal of Computer Science, 2021, 8: 145-151.

Chen L C, Zhu Y, Papandreou G, et al. Encoder-decoder with atrous separable convolution for semantic image segmentation[C]//Proceedings of the European conference on computer vision (ECCV). 2018: 801-818.

Dell'Aglio D A G, Gargiulo M, Iodice A, et al. Active fire detection in multispectral super-resolved sentinel-2 images by means of sam-based approach[C]//2019 IEEE 5th International forum on Research and Technology for Society and Industry (RTSI). IEEE, 2019: 124-127.

Ding Y, Wang M, Fu Y, et al. A wildfire detection algorithm based on the dynamic brightness temperature threshold[J]. Forests, 2023, 14(3): 477.

Gargiulo M, Dell’Aglio D A G, Iodice A, et al. A CNN-based super-resolution technique for active fire detection on Sentinel-2 data[C]//2019 PhotonIcs & Electromagnetics Research Symposium-Spring (PIERS-Spring). IEEE, 2019: 418-426.

Van Oldenborgh G J, Krikken F, Lewis S, et al. Attribution of the Australian bushfire risk to anthropogenic climate change[J]. Natural Hazards and Earth System Sciences Discussions, 2020, 2020: 1-46.

Wang J H, Li F, Lu M, et al. Multi temporal and multi-channel cloud detection algorithm based on GF-4 data [J]. Chinese Space Science and Technology, 2022,42(03): 132-140. (in Chinese).

Zhang F, Zhao P, Xu S, et al. Integrating multiple factors to optimize watchtower deployment for wildfire detection[J]. Science of the total environment, 2020, 737: 139561.